NOVEL EPDM/PARAFFIN FOAMS FOR THERMAL ENERGY STORAGE APPLICATIONS

Francesco Valentini*, Andrea Dorigato, Luca Fambri, Alessandro Pegoretti*

University of Trento, Department of Industrial Engineering and INSTM Research Unit, Via Sommarive 9
38123 Trento, Italy

ABSTRACT

The thermomechanical behavior of ethylene–propylene–diene monomer (EPDM) foams filled with different concentrations of a paraffin (melting temperature of 21 °C) are investigated for the first time. Samples were prepared by melt compounding and hot pressing, and the effects of two different foaming agents such as Expancel® 909DU80 (E) and Hostatron® P0168 (H) were investigated. Scanning electron microscopy and density measurements highlighted that the use of E foaming agent led to foams with a closed-cell morphology and a mean pore size of about 20 µm, whereas foams expanded with H were characterized by a mixed closed-/open-cell porosity with a larger cell size (of about 100 µm) and a less uniform pore distribution. Differential scanning calorimetry analysis demonstrated that the produced foams were endowed with noticeable thermal energy storage properties (up to 67 J/g with a paraffin amount of 50 wt%). The corresponding thermal parameters were found in the range of 15–50 J/cm^3, which were directly dependent on the paraffin content in both heating and cooling. The drop in the maximum tensile stress at elevated paraffin contents observed in the tensile impact tests at 23 °C was counterbalanced by a noticeable enhancement of the deformation at break and of the absorbed impact energy. Tensile tests performed at 0 °C demonstrated that the addition of paraffin within the foams was responsible for a substantial increase in stiffness, whereas at 40 °C, it plays a plasticizing effect. [doi:10.5254/rct.21.79976]

INTRODUCTION

The term *climate change* refers either to a persistent variation in the climate or to its variability. It can occur in natural processes or in external events, changing the composition of the atmosphere.[1] In the past 150 years, the energy consumption related to human activities has resulted in the accumulation of a huge amount of greenhouse gases, resulting in chemical changes in the atmosphere.[2] Alexiadis[3] showed that the CO_2 emissions related to human activities has become the main driving force in global warming. In this context, the development of energy conservation and/ or management systems could represent an efficient way to reduce global energy consumption. Energy storage systems are based on the accumulation of different forms of energy (thermal, electrical, etc.), when available, to use at a later time.[4,5]

Thermal energy storage (TES) allows the storage of thermal energy in a storage medium for heating/cooling applications. TES systems can help to balance the energy demand of buildings, reducing absorption peaks and thus reducing energy consumption and CO_2 emissions.[6,7] In this sense, latent heat TES systems are particularly attractive because they provide an elevated energy storage density at constant temperature. Because of the transition of the material involved from a physical state to another one (for example, from solid to liquid), these materials are generally called *phase-change materials* (PCMs).[8–11] Paraffins are organic PCMs characterized by low cost, high heat of fusion, a broad range of melting temperatures, low vapor pressure in the melting state, and chemical stability.[7–9] They are used for several applications, such as thermoregulated building materials,[10,12] solar energy storage devices,[13] sport equipment,[14] and smart fabrics.[15–17] The main problem related to their use is their leakage in the molten state, which requires the confinement of the PCM either by encapsulation[17,18] or by shape stabilization.[19–21] To avoid PCM flow and/or leakage, the paraffin can be encapsulated in other polymer matrices, such as polyolefins,

elastomers, and polymer blends,[22–29] thus forming a shape-stabilized PCM. Different hosting matrices such as high-density polyethylene,[30] polypropylene,[31] poly(methylmethacrylate),[32] polyurethane copolymers,[33] acrylic resins,[27] and styrene–butadiene–styrene rubber have been considered thus far in the open literature.

In the past few years, polymer foams have gained great interest because of their specific features. Because of their combination of low density and limited thermal conductivity, these materials are perfect candidates for the thermal insulation of residential, industrial, and commercial buildings.[34] Polymer foams are expanded polymers prepared by a blowing agent, and depending on the foaming parameters, they can be characterized by open-cell and/or closed-cell porosity.[35] The foaming process is generally carried out through the generation of gases within the polymer matrix generated by the thermal decomposition of a chemical blowing agent.[36] The blowing agent is generally a solid chemical (with organic or inorganic nature) that is added to the polymer matrix. Inorganic blowing agents (such as sodium and potassium carbonates) decompose endothermically and release CO_2 and water under the action of heat. Organic blowing agents, instead, decompose mainly exothermically and release nitrogen.[36]

Expanded rubbers are materials that consist of a rubber matrix and in pores containing a gas phase (generally air). Depending on the morphology of the pores (i.e., open-cell and/or closed-cell structure), these materials could be used in several applications, ranging from thermal insulation, gaskets, and impact sound–deadening products.[37,38] Rubber foams can be produced with traditional blowing agents starting from natural rubber[39,40] or synthetic rubber such as styrene–butadiene rubber,[41] acrylonitrile butadiene rubber (NBR),[42] and ethylene–propylene–diene monomer (EPDM) rubber[38] and their blends,[43] reaching density values in the range of 0.27–0.48 g/cm³. Moreover, salt leaching has also been presented for the preparation of NBR and EPDM foams.[44,45] EPDM is one of the most widely used elastomers at the industrial scale. It is a synthetic rubber made from ethylene and propylene polymerized with a nonconjugated diene monomer (typically dicyclopentadiene, 5-vinyl-2-norbornene or 5-ethylidene-2-norbornene) and can be vulcanized at an elevated temperature, usually in the range of 160–180 °C, through the formation of sulphur bridges.[46] EPDM rubber compounds can generally be obtained by mixing the base polymer with vulcanizing agents, antioxidants, activators, fillers (carbon black), and accelerators.[47] The resulting materials are generally characterized by good mechanical properties and high resistance to aging, ozone, ultraviolet light, and weathering. The main disadvantage is related to their poor resistance to polar fluids and oils. EPDM foams are mainly applied in the production of gaskets, O-rings, window profiles, belts, electrical insulation of cables, and waterproofing membranes.[48]

In the literature, only a few works can be found on the TES properties of EPDM matrices filled with different kinds of PCM, and most are focused on the use of paraffin waxes directly mixed within the EPDM matrix[11,22] or stabilized with expanded graphite.[49] The reported results confirmed the potential of paraffin as PCM within an EPDM matrix. Despite the possible advantages of the combination of an elastomeric foam filled with a PCM for thermal management applications, no studies can be found in the open literature. Moreover, the recent European requirements regarding the construction of nearly zero-energy buildings can represent a further stimulus for research in the development of innovative multifunctional materials for thermal insulation. Based on these considerations, this work investigates the most important physical, thermal, and mechanical properties of EPDM foams that contain different amounts of a paraffin wax, with a melting temperature of 21 °C (i.e., near room temperature), to verify the suitability of the use of this PCM as a TES material in an elastomeric foamed matrix. This work considers two different kinds of foaming agents and investigates the correlation between the microstructural features of the obtained foams and their thermomechanical behavior.

TABLE I

COMPOSITION OF THE ELASTOMERIC EPDM COMPOUND USED FOR THE
PREPARATION OF THE COMPOSITES

Material	Quantity, phr
Vistalon 2504	100
Sulphur	3
Zinc oxide	3
Stearic acid	1
Carbon black	20
Tetramethylthiuram disulphide	0.87
Zinc dibutyl dithiocarbamate	2.5

EXPERIMENTAL

MATERIALS

Vistalon® 2504 EPDM rubber is an amorphous terpolymer with a broad molecular weight distribution, a low Mooney viscosity (ML 1+4, 125 °C) of 25 MU, a medium diene content (4.7 wt% of ethylidene norbornene), and a low ethylene content (58 wt%); it was purchased from Exxon Mobil (Irving, TX, USA) in the form of solid dense bales. Rubitherm RT21HC is a paraffinic wax, with a melting point of 21 °C and a melting enthalpy (ΔH_m) of 139 J/g and was purchased from Rubitherm GmbH (Berlin, Germany). This PCM was selected to store/release thermal energy in a temperature interval near room temperature. Zinc oxide (curing activator), stearic acid (curing activator and lubricating agent), and sulphur (vulcanizing agent) were supplied by Rhein Chemie (Cologne, Germany). The accelerators, tetramethylthiuram disulphide and zinc dibutyl dithiocarbamate, were obtained from Vibiplast srl (Castano Primo [MI], Italy). Carbon black N550 was used as a reinforcing filler and was obtained from Omsk Carbon Group (Omsk, Russia). Organophilic montmorillonite Cloisite® 20 was obtained from BYK-Chemie GmbH (Wesel, Germany). Two different foaming agents were considered in this work: Hostatron® P0168 (H) was obtained from Clariant GmbH (Ahrensburg, Germany), whereas Expancel® 909DU80 (E) was purchased from Nouryon Chemicals Spa (Milano, Italy). The foaming agent H is a mixture of sodium, calcium, and potassium bicarbonates. The expansion occurs through the decomposition of the bicarbonates that takes place at 150 °C, and the reaction products are carbonates, CO_2, and vapor. The foaming agent E consists of microspheres containing isopentane that, when the temperature increases to greater than 130 °C, start expanding because of the vaporization of isopentane. The composition of the elastomeric compound used for the preparation of the samples in this work is reported in Table I, and the quantities are expressed in phr. Preliminary studies investigated the formulations of various EPDM compounds and the effect of different blowing agents to obtain the lowest-density values, the composition of which is reported in Table I. The results are summarized in Table II, which presents, highlighted in bold, the selected formulation of 1.3 phr of foaming agent H and 14 phr of foaming agent E.

SAMPLE PREPARATION

EPDM/paraffin blends with different paraffin contents ranging from 30 wt% (i.e. 70 wt% of EPDM compound) to 50 wt% (i.e., 50 wt% of EPDM compound) were prepared by melt compounding in an internal mixer (Thermo Haake Rheomix® 600), equipped with counter-rotating rotors. The compounding temperature was kept at 40 ± 1 °C and maintained for the entire mixing

TABLE II
RESULTS OF DENSITY MEASUREMENTS PERFORMED ON PRELIMINARY
EPDM COMPOUNDS[a]

Foaming agent	Amount, phr	Density, g/cm^3
Expancel 909DU80	12.4	0.631 ± 0.088
	14	**0.592 ± 0.098**
	14.8	0.596 ± 0.081
	16	0.613 ± 0.089
Hostatron P0168	1	0.629 ± 0.007
	1.3	**0.575 ± 0.003**
	2	0.612 ± 0.016
	2.75	0.662 ± 0.018

[a] Formulations with the lowest density (highlighted in bold) have been selected.

process, whereas the rotor speed was set at 50 rpm. First, EPDM was fed into the mixer with the carbon black and mixed for 5 min, and then the vulcanizing agent and the additives were added and mixed for another 5 min. To stabilize the PCM though nanoclay intercalation, the liquid paraffin wax was first mixed with the Cloisite 20 nanoclay (at a constant paraffin/nanoclay ratio of 3:1[50]) and then ultrasonicated for 5 min at room temperature using a Hielscher UP400S device (Teltow, Germany), equipped with a cylindrical sonotrode with a diameter of 15 mm and operating at a power of 400 W. The resulting mixture was then gradually fed into the mixer and mixed for 5 min. To produce the foams, the foaming agent was then added and mixed for 5 min, for a total mixing duration of 20 min.

The foaming and vulcanization process of the resulting compounds were carried out simultaneously under a hydraulic press at a pressure of 2 bar and a temperature of 170 °C. After 10 min, the press was opened to allow a free expansion of the material, and the samples were left for an additional 10 min to allow the completion of the vulcanization process at 170 °C. In this way, square sheets with dimensions of about $110 \times 110 \times 5$ mm^3 of the blends at different compositions were obtained. The list of the prepared foams (including their surface density, evaluated as the product of the geometrical density and the thickness of each sample) along with their codes is reported in Table III. The name of foamed rubber is composed by a first capital letter indicating the foaming agent (E for Expancel 909DU80 or H for Hostatron P0168), and then RTX0, where X0 represents the percentage by wt. of RT21HC in the compound. For example, E-RT30 means a sample foamed using Expancel 909DU80 and containing 30 wt% of RT21HC.

The surface density was also reported and expressed in kg/m^2. It is directly dependent on the material (formulation) and on the geometrical thickness (processing): the higher the bulk density, and the higher the thickness, the higher the surface density.

The sample termed *EPDM* refers to the neat EPDM rubber (surface density 4.93 kg/m^2) that was prepared by melt compounding at 40 °C: EPDM was fed into the mixer with the carbon black and mixed for 5 min, and then the vulcanizing agent and the additives were added and mixed for another 5 min. The vulcanization process was carried out at a temperature of 170 °C for 20 min, under a hydraulic press at a pressure of 8 bar, obtaining square sheets with dimensions of $110 \times 110 \times 5$ mm^3. It should be noted that it was possible to obtain foamed samples and reference samples that had the same dimensions, because the amount of material inserted in the mold was different and optimized for each foaming agent. It should also be noted that, in the case of the foamed materials, it was necessary to open the mold during the vulcanization process because the expansion occurred

TABLE III
COMPOSITION AND CODE OF THE PREPARED SAMPLES

Sample code	RT21HC (wt%), phr	Cloisite 20 (wt%), phr	Expancel 909DU80 (wt%), phr	Hostatron P0168 (wt%), phr	Surface density, kg/m^2
EPDM	—	—	—	—	4.93
E-RT0	—	—	9.7–14	—	3.09
E-RT30	30–75	7.1–16	9.7–14	—	2.87
E-RT40	40–98	9.1–24.5	9.7–14	—	2.98
E-RT50	50–174	12.0–43.5	9.7–14	—	3.16
H-RT0	—	—	—	0.99–1.3	3.68
H-RT30	30–75	7.5–16	—	0.99–1.3	4.17
H-RT40	40–98	9.6–24.5	—	0.99–1.3	3.91
H-RT50	50–174	12.4–43.5	—	0.99–1.3	4.37

mainly in the x–y direction and not in the z direction: for this reason, the thickness of the samples was 5 mm, and the main variation was in the x–y direction.

EXPERIMENTAL METHODOLOGIES

The cryofractured surfaces of the foams containing paraffin were observed through a Zeiss Supra 40 field emission scanning electron microscope (FESEM), operating at an acceleration voltage of 2.5 kV. Before being observed, the samples were metallized through the deposition of a thin, electrically conductive coating of platinum palladium inside a vacuum chamber.

Helium pycnometry density (ρ_{picn}) measurements were carried out to determine the density of the investigated materials. Tests were conducted by means of a gas displacement AccuPycII 1330 pycnometer (Micromeritics Instrument Corporation, Norcross, GA, USA) at a temperature of 23.0 °C on specimens weighing about 0.2 g. For each sample, 30 replicates were performed. A measure of the geometrical density (ρ_{geom}; i.e., mass over the total volume inclusive of solid porosity, closed porosity [CP], and open porosity [OP]) was also carried out. The geometrical density was measured on five cylindrical specimens (diameter of 10 mm) by measuring the mass with a Gibertini E42 balance (0.1 mg sensitivity) and the dimensions by means of a caliper (resolution of 0.01 mm). According to ASTM D6226 standard, it was possible to calculate the total porosity (P_{tot}) and the fraction of OP and CP according to Eqs. 1–3:

$$P_{tot} = \left(1 - \frac{\rho_{geom}}{\rho_{bulk}} \right) \times 100 \qquad (1)$$

$$OP = \left(1 - \frac{\rho_{geom}}{\rho_{picn}} \right) \times 100 \qquad (2)$$

$$CP = P_{tot} - OP \qquad (3)$$

where ρ_{bulk} is the density of the material without porosity (i.e., 0.986 g/cm^3 for the EPDM sample, similar to values present in literature[34]). In the case of materials containing paraffin, the ρ_{bulk} values were determined using the mixture law. Thermogravimetric analysis (TGA) was performed through a Q5000 IR thermobalance under a nitrogen flow of 10 mL/min in a temperature interval between 30 and 700 °C and a heating rate of 10 °C/min. The temperature associated to a mass loss of

TABLE IV
RESULTS OF DENSITY MEASUREMENTS AND POROSITY EVALUATION

Sample	ρ_{picn}, g/cm^3	ρ_{geom}, g/cm^3	ρ_{bulk}, g/cm^3	OP, %	CP, %	P_{tot}, %
EPDM	0.987 ± 0.002	0.986 ± 0.084	0.986	—	—	—
E-RT0	0.617 ± 0.002	0.592 ± 0.098	0.986	4.1	35.9	40.0
E-RT30	0.573 ± 0.008	0.480 ± 0.016	0.922	16.3	31.6	47.9
E-RT40	0.596 ± 0.007	0.516 ± 0.012	0.900	13.3	29.3	42.6
E-RT50	0.632 ± 0.011	0.592 ± 0.018	0.878	6.4	26.2	32.6
H-RT0	0.735 ± 0.005	0.575 ± 0.003	0.986	21.7	19.9	41.7
H-RT30	0.833 ± 0.017	0.568 ± 0.008	0.922	31.8	6.6	38.4
H-RT40	0.782 ± 0.015	0.596 ± 0.048	0.900	23.7	10.0	33.8
H-RT50	0.874 ± 0.007	0.734 ± 0.062	0.878	29.4	0.3	29.7

5% ($T_{5\%}$), the temperatures associated to the maximum rate of degradation (T_{peak1}, T_{peak2}, T_{peak3}), and the residual mass at 700 °C (m_{700}) were determined. Differential scanning calorimetry (DSC) measurements were performed using a Mettler DSC30 calorimeter under a nitrogen flow of 10 mL/min. A heating scan from −30 to 40 °C was followed by a cooling stage from 40 to −30 °C. All thermal ramps were carried out at 10 °C/min. In this way, the melting and crystallization temperatures (T_m, T_c) and the specific melting and crystallization enthalpy values (ΔH_m, ΔH_c) were obtained. The volumetric-specific enthalpy P was evaluated by multiplying the experimental enthalpy values by geometrical density for heating and cooling (i.e., as $P_{Heat} = \Delta H_m/\rho_{geom}$ and $P_{Cool} = \Delta H_c/\rho_{geom}$, respectively). In the case of paraffin, the density values reported in the technical data sheet were used (0.88 g/cm^3 at the solid state, 0.77 g/cm^3 at the liquid state). Moreover, the TES efficiency was determined during both the heating scan (η_m) and the cooling scan (η_c) as the ratio between the specific enthalpy of the samples and the corresponding specific enthalpy values of the neat paraffin, taking into account the PCM weight concentration within the materials, as shown in Eqs. 4–5:

$$\eta_m = \left(\frac{\Delta H_m}{\Delta H_{mPCM} \times wt\%_{PCM}} \right) \times 100 \qquad (4)$$

$$\eta_c = \left(\frac{\Delta H_c}{\Delta H_{cPCM} \times wt\%_{PCM}} \right) \times 100 \qquad (5)$$

where ΔH_{mPCM} and ΔH_{cPCM} are, respectively, the specific enthalpy values associated with the melting and crystallization of the neat PCM, whereas $wt\%_{PCM}$ is the PCM content within the blends.

Tensile properties under quasi-static conditions were measured on ISO 527 type 1BA specimens, 5 mm in thickness, through an Instron 5969 tensile testing machine (Instron, Norwood, MA, USA) equipped with a load cell of 10 kN. Tensile tests at break were performed at a cross-head speed of 100 mm/min at temperature levels below 0 °C and above 40 °C, the melting point of the PCM. The elastic modulus was measured as a secant value between strain levels of 0.05% and 0.25%; moreover, the maximum tensile strength and the corresponding strain levels were determined. At least five specimens were tested for each composition. To consider the effect of the porosity within the foamed samples, the resulting tensile properties were normalized for the geometrical density of the foams, whose value are reported in Table IV. Tensile impact tests were performed at 23 °C by using an instrumented CEAST impact machine (Instron) equipped with a 2.54 kg mass striker at an impact speed of 2.2 m/s. ISO 527 type 1BA dog-bone specimens 5 mm in
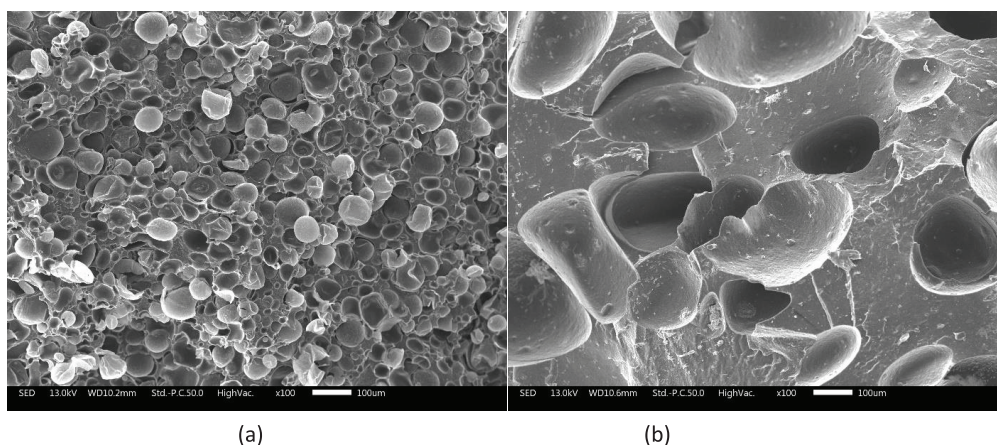
FIG. 1. — SEM micrographs of (a) E-RT0 and (b) H-RT0 samples (100×).

thickness were used, and at least five specimens for each composition were tested. In this way, the maximum stress and the total absorbed energy under impact conditions were determined. Even in this case, the impact properties were normalized for the density of the foams. In this case, the total absorbed energy values were also normalized for the cross section of the specimens.

RESULTS AND DISCUSSION

Considering that the thermomechanical properties of the foams are strictly related to their morphology, FESEM observations were carried out to investigate the morphological features of the produced foams and to assess the dispersion degree of paraffin wax within the elastomeric matrix. The FESEM micrographs of the E-RT0 and H-RT0 samples presented in Figure 1a,b highlight the different morphologies determined by the use of the two foaming agents.

It can be observed that the foaming agent E (Expancel) led to the formation of closed-cell pores distributed homogenously within the matrix, with a mean size of about 20 μm. On the other hand, the porosity obtained using the foaming agent H (Hostatron) was completely different: in this case, the pores were not distributed homogenously within the EPDM matrix, and the size of the pores was considerably higher (about 100 μm). This difference could play a key role in the thermomechanical properties of the produced foams. Comparing the FESEM micrographs of E-RT0 and E-RT40 samples presented in Figure 2a–d, it is possible to observe that the addition of paraffin did not substantially influence the porosity and the pore size within the EPDM. It can also be noticed that the paraffin domains were uniformly distributed within the elastomeric matrix, without occluding the pores in the materials.

It is clear that the morphology of the foams was strictly connected to their density and porosity. Therefore, density measurements were performed, along with determination of the relative amounts of OP, CP, and total porosity. The density measurements reported in Table IV show that foaming agent E led mainly to the formation of a closed-cell porosity and to lower density values than those obtained with foaming agent H. This behavior is due to the fact that the foaming agent E is constituted by microcapsules containing low-boiling-point hydrocarbons: because the expansion is due to the expansion of the microspheres, the porosity is mainly closed. In the case of H foaming agent, the expansion is due to the production of CO_2 and vapor, which lead to the formation of porosity with either an open or closed cell. Moreover, it can be noticed that the minimum values of density were obtained after the addition of about 30 wt% of paraffin using H and E foaming agent; a
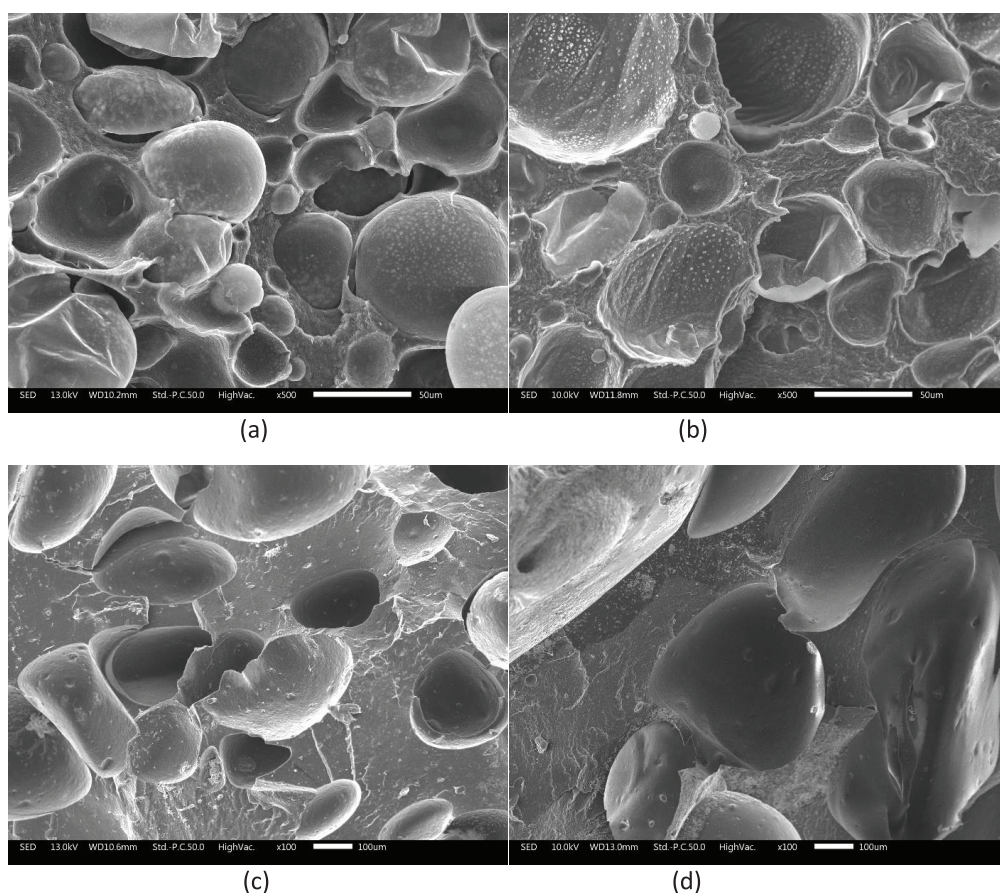
FIG. 2. — SEM micrographs of samples (a) E-RT0 (500×), (b) E-RT40 (500×), (c) H-RT0 (100×), and (d) H-RT40 (100×).

further increase of the paraffin content did not lead to a further decrease in density, whereas the P_{tot} values continued to decrease linearly with the paraffin content. This behavior can be attributed to the plasticizing effect of paraffin,[51] which causes changes in the consistency of EPDM rubber characterized by low resistance to oils. The samples containing 40 and 50 wt% of RT21HC, before the vulcanization, were characterized by the consistency of a very sticky slurry that probably hindered the expansion ability of the samples, impairing the microcapsule expansion (in the case of the E foaming agent) and the release of gases (in the case of the H foaming agent).

Considering the possibility of using the prepared foams as thermal insulating materials in the building sector, it is clear that the foams produced with E could be more suitable for achieving lower thermal conductivity values, because of the lower pore size and the higher CP and P_{tot} values.[52] Further investigation will be performed in the future to measure the thermal conductivity of the prepared foams.

To assess the influence of the addition of paraffin and of the foaming process on the degradation resistance of the prepared materials, the investigation of the thermal degradation behavior of the prepared materials was carried out through thermogravimetric tests. The thermogravimetric curves of the bulk EPDM, of the foamed samples at different paraffin amounts, and of the neat PCM are presented in Figure 3a,b along with the corresponding derivative curves. The most significant results obtained from these tests are summarized in Table V.
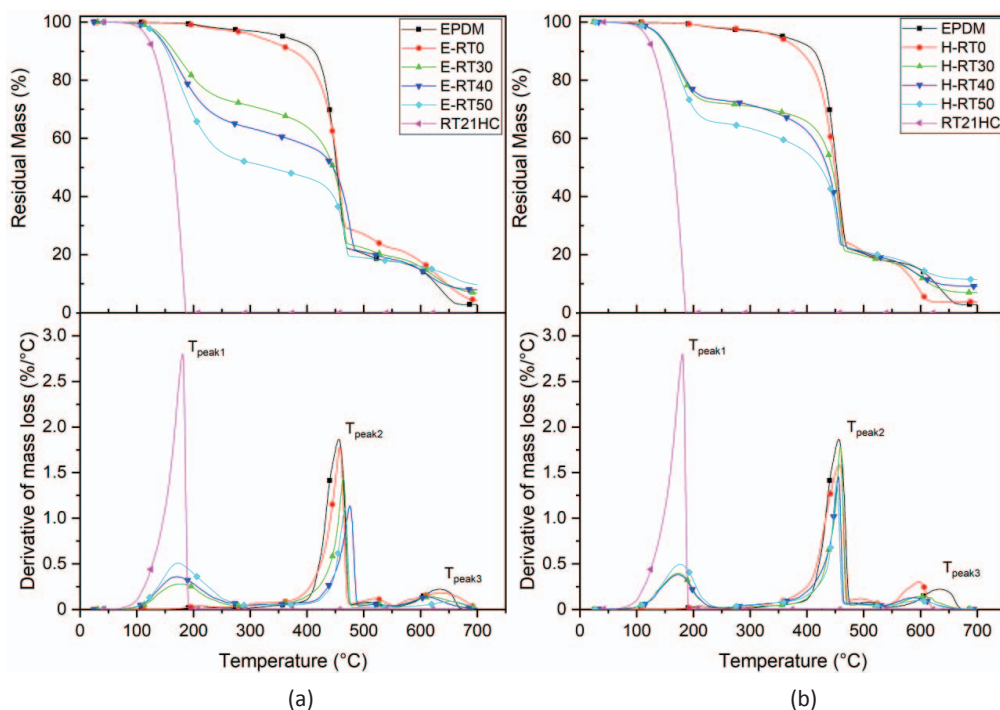
FIG. 3. — TGA curves of bulk EPDM sample, neat paraffin (RT21HC), and foams produced with different amounts of (a) E and (b) H, as foaming agent.

From the thermogram of the neat PCM sample, it is evident that the degradation took place in a single step at about 180 °C (corresponding to T_{peak1}), whereas the neat EPDM sample showed two main degradation steps, which were associated with the degradation of the polymer matrix at about 450 °C (T_{peak2}) and to the decomposition of the carbonaceous fillers at 630 °C (T_{peak3}). The TGA curves highlight that the influence of both foaming agents on the thermal stability of the EPDM matrix was very limited, as the behavior of E-RT0 and H-RT0 samples was very similar to that of the reference material, until a temperature of 300 °C. A slight shift of the mass loss curves toward the

TABLE V
RESULTS OF TGA TESTS ON THE PREPARED SAMPLES

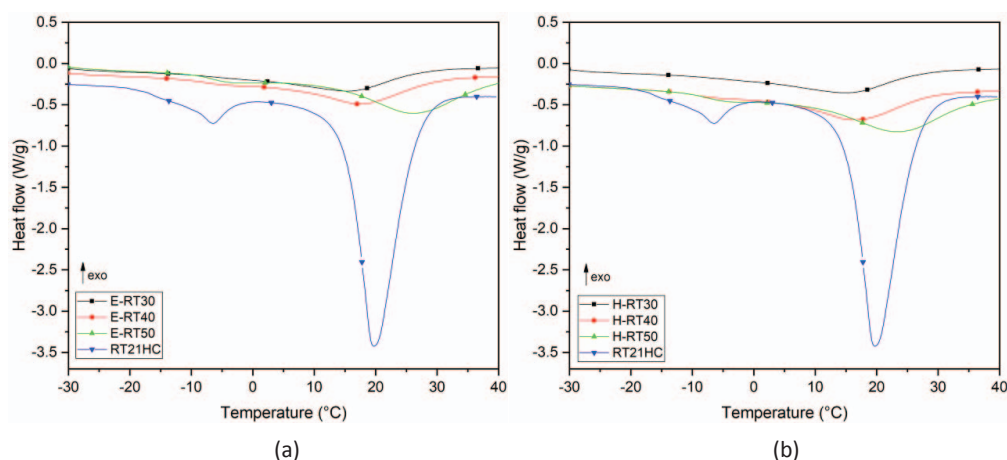| Sample	$T_{5\%}$, °C	T_{peak1}, °C	T_{peak2}, °C	T_{peak3}, °C	m_{700}, %
EPDM	359.2	—	456.1	632.8	2.87
RT21HC	117.8	180.7	—	—	0.00
E-RT0	313.3	—	457.8	641.5	4.36
E-RT30	145.2	178.1	464.1	620.1	6.82
E-RT40	139.5	170.2	475.4	611.6	7.87
E-RT50	137.2	172.5	467.0	654.7	9.74
H-RT0	397.9	—	456.6	597.2	3.77
H-RT30	140.9	172.6	458.7	607.9	6.95
H-RT40	142.5	172.3	455.3	587.4	9.08
H-RT50	139.8	176.3	452.2	592.1	11.44

FIG. 4. — DSC thermograms (heating scan) of neat paraffin (RT21HC) and foams produced with (a) E and (b) H, as foaming agents.

lower temperature was detected only at higher temperatures. This is not surprising, as it is well known that the thermal stability at an elevated temperature of the foams is generally lower than that of the corresponding bulk material, because of the increase in the surface area exposed to degradation.[53] On the other hand, it is evident that the addition of paraffin led to a gradual decrease in the thermal stability of the materials. Looking at the results summarized in Table V, it is possible to observe that the $T_{5\%}$ values of the EPDM/paraffin foams were strongly lower than that of the EPDM sample (both in bulk and in foamed form). Moreover, the decrease in the $T_{5\%}$ was proportional to the paraffin amount. It is also important to underline that the thermal degradation behavior of the samples foamed using the two different foaming agents was very similar, because the difference in the T_{peak2} values of the samples with the same paraffin amount was not so pronounced. Only a slight decrease in the T_{peak2} values could be observed in the samples foamed with H in comparison with the foams produced with E. At high testing temperatures, the behavior of the foams was very similar to that of the reference EPDM compound, and even in this case, foams with H agent showed T_{peak3} values lower than those of E-foamed materials. Looking at the residue at 700 °C (m_{700}), the neat paraffin sample completely degraded without leaving any solid residue, whereas for the other samples, it was about 5–10 wt%; in general, higher values were reached in the case of foamed samples containing paraffin. The increase in the m_{700} values for the samples containing paraffin was due to the presence of Closite20, which was added as a shape stabilizer for paraffin at a constant paraffin/nanoclay ratio of 3:1. As reported in Table III, this amount, with respect to the total sample mass, corresponds to about 7 wt% in the case of H-RT30 and E-RT30, 9 wt% in the case of H-RT40 and E-RT40, and 12 wt% in the case of H-RT50 and E-RT50; the composition percentages are coherent with the residual mass m_{700} values reported in Table V.

To investigate the role of the foaming process and of the addition of paraffin on the thermal properties of the blends, DSC tests were performed. The DSC thermograms collected in the first heating scan are presented in Figure 4a,b, whereas the most important results obtained from these tests in the first heating and in the cooling scan are collected in Table VI.

From these thermograms, the presence in the foam of the melting peak of the PCM at about 20 °C was evident, whose intensity was proportional to the paraffin amount. The secondary melting peak of the paraffin in the range −15 to 0 °C (about 11 J/g) was not detectable in the foamed systems.

Compositions at 30 wt% of PCM exhibited a less pronounced melting peak than pure paraffin, with a lower melting temperature (T_m) and lower crystallinity. On the other hand, it is also worth

TABLE VI
RESULTS OF DSC TESTS ON NEAT PARAFFIN (RT21HC) AND THE PREPARED FOAMS (HEATING SCAN AND COOLING SCAN)

Sample	T_m, °C	ΔH_m, J/g	P_{heat}, J/cm^3	η_m, %	T_c, °C	ΔH_c, J/g	P_{cool}, J/cm^3	η_c, %
RT21HC	19.4	139.1	107.1	100.0	12.9	149.7	131.7	100.0
E-RT30	15.5	31.1	14.9	74.5	−7.5	31.3	15.0	69.7
E-RT40	17.5	42.5	21.9	76.4	−2.1	42.4	21.9	70.8
E-RT50	26.0	63.1	37.4	90.7	−2.2	62.9	37.2	84.0
H-RT30	15.1	37.8	21.5	90.6	−6.7	36.8	20.9	81.9
H-RT40	16.4	50.5	30.1	90.8	−0.7	50.0	29.8	83.5
H-RT50	23.2	67.2	49.3	96.6	−0.1	65.6	48.2	87.6

noting that at higher paraffin amounts, the shift of the T_m values toward higher temperatures was attributed to the lower thermal conductivity of the foamed EPDM matrix. For the same reason, the T_c values of the foams were systematically lower (up to 20 °C of difference) than those shown by the RT21HC sample, depending on the physical constrains and lower nucleation effects in the foamed systems. The difference in temperature, either in melting or in crystallization, was more pronounced in the case of E-RT30 and H-RT30 samples with respect to the corresponding materials containing 50 wt% of paraffin. This behavior in cooling can be determined by the lower thermal conductivity of the EPDM rubber foam with respect to paraffin, which consequently reduces the crystallization kinetics of the paraffin. Moreover, at a higher paraffin content (40 and 50%), the undercooling was less pronounced because of the lower relative content of the foamed rubber. An analogous behavior was also observed for PCM microcapsules dispersed in acrylic matrix and carbon–fiber composites with higher melting temperature and lower crystallization temperature than single PCM microcapsules.[54]

In analyzing ΔH_m and ΔH_c values, all prepared foams showed an interesting TES capability, in both heating and cooling. The melting and crystallization enthalpy values were proportional to the amount of paraffin. For instance, a ΔH_m value of 67 J/g could be obtained for the H-RT50 sample. Moreover, in view of the applications, the volumetric thermal parameter of the produced foams, either in heating (P_{Heat}) or in cooling (P_{Cool}), was found in the range of 15–50 J/cm^3, which was almost linearly dependant on the composition of the H-foamed systems, analogously to the values of 27–47 J/cm^3 of epoxy-laminated composites reported by Fredi et al. in 2018.[55]

Considering the TES efficiency, it can be seen that the efficiency values detected in the first heating scan were greater than 75% for all samples and that η_m values of the foams prepared with the H-foaming agent were systematically higher than those shown by E-foamed materials. This could be explained by the reduction in paraffin leakage during the expansion process because of the lower expansion efficiency of foaming agent H. For the H-50 sample, a η_m value of 96.6% was detected. The same conclusions can be drawn if the efficiency values obtained in the cooling scan (η_c) are considered. This means that the PCM stabilization through the addition of nanoclay was able to prevent the thermal degradation of the paraffin during the melt compounding and its leakage during the foaming operations. We observed a similar effect in our previous paper on epoxy samples, in which paraffin wax was stabilized with carbon nanotubes.[21] In another work on polyamide 12 thermoplastic composites, in which a paraffin wax was stabilized with carbon nanotubes, the authors observed that both melt-compounding and hot-pressing operations led to a significant lowering of the TES efficiency values, especially at higher amounts of PCM.[17] This probably means that the mild processing conditions applied during the compounding operations in the present work (i.e., 40 °C at 50 rpm for 8 min) prevent the leakage and degradation of the paraffin, thus retaining the TES capability of the prepared foams. It should be noted that the secondary
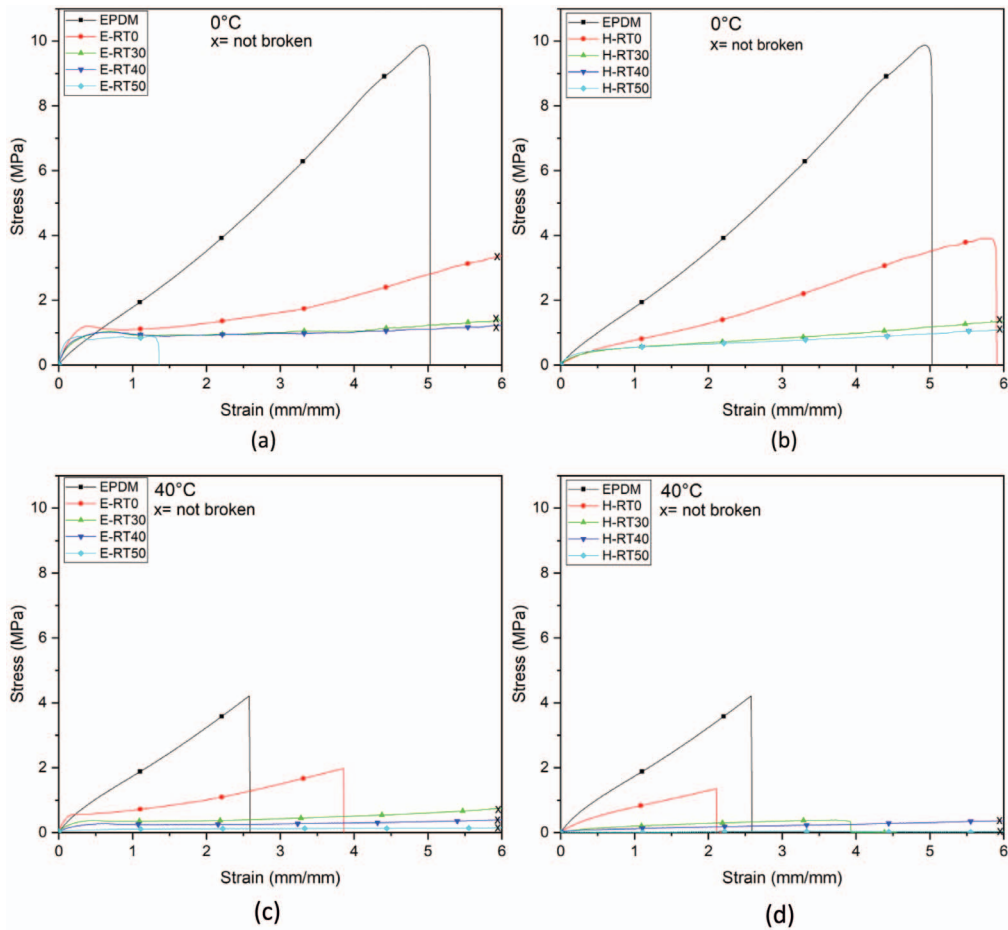
FIG. 5. — Stress–strain curves at 0 °C and 40 °C of bulk EPDM samples and of foams produced with (a, c) E and (b, d) with H, as foaming agents.

endothermic peak of paraffin at about −10 °C is also present in the cooling and in the second heating scan with the same enthalpic values; further investigations will be carried out to interpret this behavior and the absence in the foamed systems.

Quasi-static tensile tests were carried out at 0 and 40 °C to quantify the influence of the addition of paraffin on the mechanical properties of the compounds below and above the melting temperature of the PCM, respectively. Figure 5a–d presents the stress–strain curves at 0 °C and 40 °C of the bulk EPDM sample and of the foams obtained with both foaming agents. As expected, the mechanical properties of the samples at 0 °C were systematically higher than those obtained at 40 °C. The neat EPDM sample behaves like a typical elastomeric compound, with a sudden drop in the sustained load after maximum tensile stress. It is also interesting to note that for all foamed samples filled with paraffin, it was not possible to detect the failure at strain levels up to 600%.

In analyzing the numerical results of the tests performed at 0 °C (listed in Table VII), it is interesting to note that the addition of PCM led to an impressive increase in the elastic modulus, proportionally to the PCM amounts. It can be suggested that the elastic modulus of the paraffin at 0 °C is therefore higher than that of the EPDM matrix. From the results of the tests carried out at 40 °C (see Table VIII), it seems that the introduction of paraffin in the liquid state leads to a strong decrease

TABLE VII

RESULTS OF QUASI-STATIC TENSILE TESTS AT 0 °C ON THE PREPARED SAMPLES

Sample	E^*, MPa·cm^3/g	σ_{max}^*, MPa·cm^3/g	ε_{max}, %
EPDM	3.33 ± 0.62	12.01 ± 2.77	492 ± 92
E-RT0	15.17 ± 4.16	4.37 ± 1.16	>600
E-RT30	21.42 ± 2.76	3.37 ± 0.57	>600
E-RT40	23.48 ± 1.77	2.52 ± 0.26	>600
E-RT50	39.31 ± 2.21	0.80 ± 0.10	>600
H-RT0	3.28 ± 0.58	5.58 ± 0.43	558 ± 79
H-RT30	8.37 ± 0.77	2.78 ± 0.22	>600
H-RT40	11.86 ± 1.82	2.01 ± 0.29	>600
H-RT50	41.28 ± 10.33	1.21 ± 1.08	>600

in the elastic modulus that, in the case of the H-RT30 and H-RT40 samples, is lower than that of the EPDM sample, whereas for E-RT30 and E-RT40, it is still slightly higher. Moreover, it is possible to observe that the values of the elastic modulus for the H-RT0 and E-RT0 samples differed strongly, at both 0 °C and at 40 °C; in particular, H-RT0 presented values similar to that of the EPDM sample, whereas the E-RT0 sample exhibited higher values. This behavior can be attributed to the higher stiffness of the microcapsules containing the E foaming agent, with respect to the neat EPDM rubber. The presence of paraffin, as already observed, changes the values of the elastic modulus, but the trend remains almost analogous. In particular, the H samples are characterized by much lower values of elastic modulus with respect to E samples because of the substantial differences in the matrix behavior derived from the presence of the microcapsules.

At 0 °C, the addition of paraffin systematically lowers the mechanical resistance of the samples, perhaps because of the lack of the interfacial adhesion between the EPDM and the paraffin phase. Future studies should investigate this aspect in more detail. From the results of the tests carried out at 40 °C, it seems that the introduction of the paraffin at the liquid state and at elevated concentrations leads to a consistent lowering of the quasi-static tensile properties of the foams (the properties of the H-RT50 sample were too low to be determined). Considering that the foams filled with paraffin cannot be broken at deformation levels until 600%, it seems that the introduction of paraffin in the liquid state acts as a plasticizing agent within the material, thus increasing the strain at break values of the prepared foams. Moreover, it is also possible to observe that the foams produced using the E-foaming agent exhibit in general higher mechanical properties than those produced with H additive,

TABLE VIII

RESULTS OF QUASI-STATIC TENSILE TESTS AT 40 °C ON THE PREPARED SAMPLES

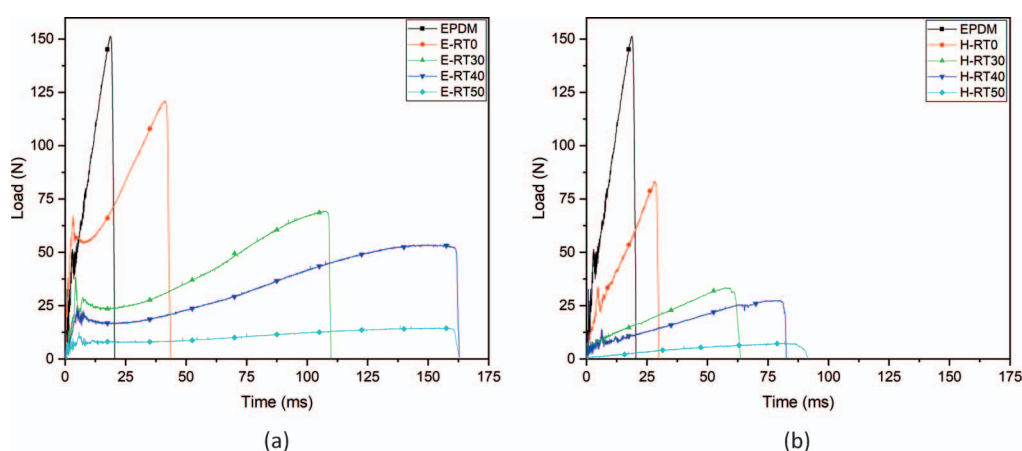| Sample	E^*, MPa·cm^3/g	σ_{max}^*, MPa·cm^3/g	ε_{max}, %
EPDM	3.54 ± 0.93	4.87 ± 1.27	273 ± 22
E-RT0	11.04 ± 3.48	3.57 ± 1.02	392 ± 56
E-RT30	6.89 ± 1.15	1.63 ± 0.51	>600
E-RT40	4.92 ± 1.35	1.02 ± 0.23	>600
E-RT50	1.84 ± 1.06	0.35 ± 0.09	>600
H-RT0	3.54 ± 0.59	2.20 ± 0.41	206 ± 35
H-RT30	1.02 ± 0.20	0.70 ± 0.20	>600
H-RT40	1.18 ± 0.96	0.57 ± 0.18	>600

FIG. 6. — Representatives curves from tensile impact tests at 23 °C on bulk EPDM samples and foams produced with (a) E and (b) H, as foaming agents.

regardless of the testing temperature. This behavior can be ascribed to the different morphology of the two foams. In fact, in the FESEM micrographs presented in Figure 1a,b, we observed that the E-RT0 foam is characterized by a microstructure with lower size pores distributed homogeneously within the rubber matrix. In these conditions, a more homogenous distribution of the stress around the pores can be obtained.

Finally, tensile impact tests were carried out at 23 °C to assess the influence of the foaming agents and of the addition of paraffin on the impact properties of the materials. Representative load-time curves are presented in Figure 6a,b, whereas the most representative results are summarized in Table IX.

Once again, the expansion of the EPDM matrix results in a general lowering of the stiffness and of the maximum impact stress, while the deformation at break is increased. This explains why the total absorbed energy of both the E-RT0 and H-RT0 samples is higher than that of the bulk EPDM sample. In fact, the total impact energy passes from 33.9 J·cm/g for the EPDM sample up to 67.4 J·cm/g for the E-RT0 sample.

In addition, in this case, it is evident the different behavior of the H-RT0 and E-RT0 samples, in particular the E-RT0, is characterized by a higher specific impact strength and higher total absorbed

TABLE IX
RESULTS OF TENSILE IMPACT TESTS AT 23 °C ON THE PREPARED SAMPLES

Sample	Specific impact strength, MPa·cm^3/g	Total specific absorbed energy, J·cm/g
EPDM	6.3 ± 2.2	34 ± 24
E-RT0	8.0 ± 1.7	67 ± 19
E-RT30	5.5 ± 0.7	104 ± 11
E-RT40	3.8 ± 0.4	105 ± 19
E-RT50	1.2 ± 0.2	39 ± 16
H-RT0	6.1 ± 0.4	34 ± 3
H-RT30	2.7 ± 0.3	40 ± 9
H-RT40	2.6 ± 0.8	41 ± 12
H-RT50	1.0 ± 0.7	18 ± 13

energy with respect to the H-RT0 (as in the case of quasi-static tests showing properties similar to those of neat EPDM rubber). This difference in behavior can be explained by the presence of the capsules in the E-RT0 that cause an increase in the stiffness of the rubber matrix but also by the different porosity that characterizes the two materials. E-RT0 is characterized by a closed-cell porosity (filled by microcapsules) that, with respect to the mixed open-cell–closed-cell porosity of the H-RT0 (not filled by microcapsules), will lead to higher impact performances.

The addition of paraffin in the foams leads to a decrease in the maximum impact stress, which is associated with a progressive enhancement of the total absorbed energy at a paraffin concentration of up to 40 wt%. When the PCM content reaches 50 wt%, a further lowering of the sustained stress occurs, leading to a decrease in the absorbed energy. It can thus be hypothesized that the paraffin in the liquid state acts as a plasticizing agent within the prepared foams, thus increasing the impact resilience of the samples. Once again, samples foamed with the E foaming agent showed higher impact properties than those in which H was adopted. As already explained, this difference could be ascribed to the finer and more homogenous pore distribution achievable with the E foaming agent.

CONCLUSIONS

The authors have reported for the first time the preparation and the thermomechanical characterization of EPDM/paraffin foams. SEM micrographs and density measurements of the prepared foams showed that the foaming agent Expancel 909DU80 (E) led to the formation of a homogeneous closed-cell morphology with pore dimensions of about 20 μm, whereas with Hostatron P0168 (H), foams with a larger cell size (of about 100 μm) with less uniform distribution could be obtained. In the latter case, a mixed closed-cell/open-cell porosity was detected. The results of the TGA highlighted that the thermal degradation resistance of the foams was progressively impaired on paraffin addition, especially in the initial degradation stages. DSC tests highlighted that the prepared foams were characterized by good TES properties, especially at elevated PCM amounts. TES efficiency values near 100% were obtained, especially with the H-foamed samples.

Tensile tests under quasi-static conditions showed that the addition of paraffin had a different influence on the produced foams below 0 °C and above 40 °C the melting temperature. At 0 °C, the addition of PCM led to a notable increase in stiffness, whereas at 40 °C, paraffin acted as a plasticizing agent. Tensile impact tests at ambient temperature demonstrated that the drop in the maximum sustained stress at elevated paraffin concentrations was counterbalanced by a significant increase in the deformation at break and thus of the total absorbed impact energy. In general, E-foamed samples showed better mechanical performance in comparison with the corresponding H-foamed materials, and this result was directly correlated to the different morphology of the foams. Therefore, this work demonstrated the possibility of preparing novel multifunctional rubber foams, which could be effectively used for thermal management applications in the building sector. The object of future research will be the study of the reproducibility and constancy of the thermal properties of various systems in different sequential heating–cooling cycles.

REFERENCES

[1]S. VijayaVenkataRaman, S. Iniyan, and R. Goic, *Renewable & Sustainable Energy Reviews* **16**, 878 (2012).

[2]I. Karakurt, G. Aydin, and K. Aydiner, *Renewable Energy* **39**, 40 (2012).

[3]A. Alexiadis, *Ecol. Model*. **203**, 243 (2007).

[4]M. R. Anisur, M. H. Mahfuz, M. A. Kibria, R. Saidur, I. H. S. C. Metselaar, and T. M. I. Mahlia, *Renewable & Sustainable Energy Reviews* **18**, 23 (2013).

[5]D. Fernandes, F. Pitié, G. Caceres, and J. Baeyens, *Energy* **39**, 246 (2012).

[6]P. Meshgin, Y. Xi, and Y. Li, *Construct. Build. Mater*. **28**, 713 (2012).

[7]H. Bo, V. Martin, and F. Setterwall, *Energy* **29**, 1785 (2004).

[8]S. Peng, A. Fuchs, and R. A. Wirtz, *J. Appl. Polym. Sci*. **93**, 1240 (2004).

[9]H. Bo, E. M. Gustafsson, and F. Setterwall, *Energy* **24**, 1015 (1999).

[10]A. M. Borreguero, M. Carmona, M. L. Sanchez, J. L. Valverde, and J. F. Rodriguez, *Appl. Therm. Eng*. **30**, 1164 (2010).

[11]A. Dorigato, M. V. Ciampolillo, A. Cataldi, M. Bersani, and A. Pegoretti, Rubber Chem. Technol. **90**, 575 (2017).

[12]C. Castellon, M. Medrano, J. Roca, L. F. Cabeza, M. E. Navarro, A. I. Fernandez, A. Lazaro, and B. Zalba, *Renewable Energy* **5**, 2370 (2010).

[13]A. Sharma, V. V. Tyagi, C. R. Chen, and D. Buddhi, *Renewable & Sustainable Energy Reviews* **13**, 318 (2009).

[14]D. Rigotti, A. Dorigato, and A. Pegoretti, *Materials Today Communications*. **15**, 228 (2018).

[15]E. Fallahi, M. Barmad, and M. Haghighat Kish, *Iran. Polym. J*. **19**, 277 (2010).

[16]F. Salaün, E. Devaux, S. Bourbigot, and P. Rumeau, *Thermochim. Acta* **506**, 82 (2010).

[17]G. Fredi, A. Dorigato, and A. Pegoretti, *eXPRESS Polym. Lett*. **12**, 349 (2018).

[18]G. Fredi, S. Dirè, E. Callone, R. Ceccato, F. Mondadori, and A. Pegoretti, *Materials* **12**, 1286 (2019).

[19]S. Phadungphatthanakoon, S. Poompradub, and S. P. Wanichwecharungruang, *Appl. Mater. Interfaces* **3**, 3691 (2011).

[20]A. Dorigato, P. Canclini, S. H. Unterberger, and A. Pegoretti, *eXPRESS Polym. Lett*. **11**, 738 (2017).

[21]G. Fredi, A. Dorigato, L. Fambri, and A. Pegoretti, *Polymers* **9**, 405 (2017).

[22]G. Song, S. Ma, G. Tang, Z. Yin, and X. Wang, *Energy* **35**, 2179 (2015).

[23]C. Alkan, K. Kaya, and A. Sari, *J. Polym. Environ*. **17**, 254 (2009).

[24]W.-I. Cheng, R.-m. Zhang, K. Xie, N. Liu, and J. Wang, *Solar Energy Materials and Solar Cells* **94**, 1636 (2010).

[25]H. Inaba and P. Tu, *Heat Mass Transfer* **32**, 307 (2019).

[26]K. Kaygusuz and A. Sari, *Energy Sources, Part A: Recovery, Utilization, and Environmental Effects* **29**, 261 (2007).

[27]K. Kaygusuz, C. Alkan, A. Sari, and O. Uzun, *Energy Sources, Part A: Recovery, Utilization, and Environmental Effects* **30**, 1050 (2008).

[28]W. Mhike, W. W. Focke, J. P. Mofokeng, and A. S. Luyt, *Thermochim. Acta* **572**, 75 (2012).

[29]M. Xiao, B. Feng, and K. Gong, *Energy Conversion and Management* **43**, 103 (2002).

[30]Y. Hong and G. Xin-shi, *Solar Energy Materials and Solar Cells* **64**, 37 (2000).

[31]I. Krupa, G. Mikova, and A. S. Luyt, *Eur. Polym. J*. **43**, 895 (2007).

[32]A. Sari, C. Alkan, A. Karaipekli, and O. Uzun, *J. Appl. Polym. Sci*. **116**, 929 (2009).

[33]Q. Cao and L. Pengsheng, *Eur. Polym. J*. **42**, 2931 (2006).

[34]B. Q. Wang, Z. L. Peng, Y. Zhang, and Y. X. Zhang, *Plastics, Rubber and Composites* **35**, 360 (2006).

[35]A. Vahidifar, S. N. Khorasani, C. B. Park, H. E. Naguib, and H. A. Khonakdar, *Ind. Eng. Chem. Res*. **55**, 2407 (2016).

[36]J. Stehr, *Gummi Fasern Kunststoffe* **68**, 821 (2015).

[37]E. Wimolmala, K. Khongnual, and N. Sombatsompop, *J. Appl. Polym. Sci*. **114**, 2816 (2009).

[38]W. Yamsaengsung and N. Sombatsompop, *J. Macromol. Sci. B* **47**, 967 (2008).

[39]M. A. Bashir, M. Shahid, R. A. Alvi, and A. G. Yahya, *Key Eng. Mater*. **510–511**, 532 (2012).

[40]J.-H. Kim, K.-C. Choi, and J.-M. Yoon, *J. Ind. Eng. Chem*. **12**, 795 (2006).

[41]S.-S. Choi, B.-H. Park, and H. Song, *Polym. Adv. Technol.* **15**, 122 (2004).

[42]A. El Lawindy, K. El-Kade, W. Abd Mahmoud, and H. Hassa, *Polym. Int.* **51**, 602 (2002).

[43]F. Deng, H. Jin, L. Zhang, and Y. He, *J. Elastom. Plast.* **20**, 1 (2020).

[44]W. Trakanpruk and Y. Rodthong, *J. Metals Mater. Miner.* **18**, 33 (2008).

[45]E. Zonta, F. Valentini, A. Dorigato, L. Fambri, and A. Pegoretti, *Polym. Eng. Sci*, **61**, 136 (2021).

[46]M. S. Sohn, K. S. Kim, S. H. Hong, and J. K. Kim, *J. Appl. Polym. Sci*. **87**, 1595 (2003).

[47]C. Komalan, K. E. George, P. A. S. Kumar, K. T. Varughese, and S. Thomas, *eXPRESS Polym. Lett*. **10**, 641 (2007).

[48]S. Datta, "Synthetic Elastomers," in *Rubber Technologist's Handbook*, J. R. White, S. K. De, Eds., Rapra Technology Ltd, Akron, OH, 2001.

[49]Y. Chen, S. Gao, C. Liu, Y. Situ, J. Liu, and H. Huang, *Solar Energy Materials and Solar Cells* **200** 109988 (2019).

[50]D. A. Ribeiro de Souza, Trento, Italy. Private communication, 2019.

[51]H. Bashir, A. Linares, and J. L. Acosta, *J. Polym. Sci. B Polym. Phys*. **39**, 1017 (2001).

[52]F. X. Alvarez, D. Jou, and A. Sellitto, *Appl. Phys. Lett*. **97**, 033103 (2010).

[53]A. Pegoretti, A. Dorigato, A. Biani, and M. Slouf, *J. Mater. Sci*. **51**, 3907 (2016).

[54]G. Fredi, A. Dorigato, and A. Pegoretti, *Polym. Compos*. **40**, 3711 (2019).

[55]G. Fredi, A. Dorigato, L. Fambri, and A. Pegoretti, *Compos. Sci. Technol*. **158**, 101 (2018).